

Domain Switching in Twisted Double Bilayer Graphene

CNF Summer Student: Peter Golemis

Student Affiliation: Physics and Electrical & Computer Engineering, University of Illinois Urbana-Champaign

Summer Program(s): 2025 Cornell NanoScale Facility Research Experience for Undergraduates (CNF REU) Program

Principal Investigator(s): Kenji Yasuda

Mentor(s): Daniel Brandon

Primary Source(s) of Research Funding: National Science Foundation under Grant No. NNCI-2025233

Contact: kenji.yasuda@cornell.edu, db923@cornell.edu, golemis3@illinois.edu

Summer Program Website(s): <https://cnf.cornell.edu/education/reu>

Research Group Website: <https://www.yasudalab.org/home>

Primary CNF Tools Used: Oxford 81 RIE, SC4500 Odd-Hour Evaporator, Zeiss Supra SEM, Nabity Nanometer Pattern Generator System

Abstract:

For over two decades, the properties of two-dimensional (2D) graphene films have been rigorously explored, exhibiting a variety of profound electronic phenomena [1]. Few-layer graphene has received great attention due to the wide range of electronic band structures realized across its various stacking orders [2]. Different coexisting stacking orders are obtained by precisely controlling the twist angle between two bilayer graphene flakes, generating Bernal (ABAB) and rhombohedral (ABCA) domains. In this work, we obtain transport measurements of small-angle twisted double bilayer graphene (TDBG) Hall bar devices with this domain structure, which exhibit gate-tunable domain switching. This platform enables the observation of the interplay between domain switching and the electronic properties of Bernal and rhombohedral graphene.

Summary of Research:

Device Fabrication:

Bernal (Fig. 1a) and rhombohedral (Fig. 1b) ordered graphene are two possible stacking configurations of four-layered graphene systems. Introducing a small twist angle between two bilayer graphene films enables the formation of large coexisting Bernal and rhombohedral domains. The electronic properties of small-angle TDBG are probed in double-gated stacks (Fig. 1c) constructed using a PDMS/PC dry transfer process. High-quality uniform gates consisting of a thin hexagonal boron nitride (hBN) dielectric and conducting graphite flake are used to tune the carrier density and out-of-plane displacement field through the TDBG. Initially, the bottom gate is stacked and placed onto a pre-patterned Si/SiO₂ substrate (Fig. 1d). Mechanically exfoliated bilayer graphene flakes are then identified using optical

microscopy and cut into two pieces by applying a high-frequency alternating voltage to a conductive atomic force microscope (AFM) tip [3].

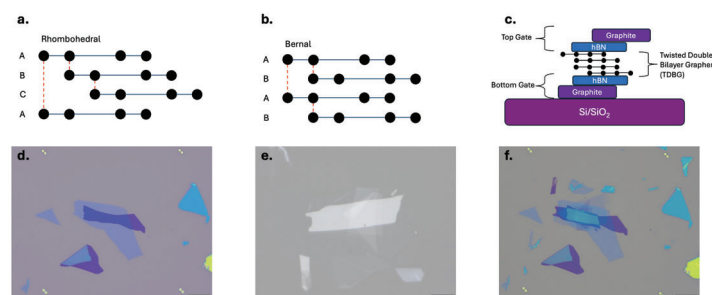


Figure 1: a, b, Visualization of rhombohedral and Bernal stacking orders in TDBG. c, Profile schematic of a double gated TDBG stack. d, Bottom gate placed on a pre-patterned chip. e, Complete top stack on PDMS/PC stamp. f, Complete stack consisting of a bottom gate (Fig. 1d) and top stack (Fig. 1e).

Scanning the conductive AFM tip over a graphene flake in a humid environment drives an anodic oxidation process to selectively remove regions of the flake with minimal induced strain on the crystal lattice. Implementing the dry transfer process, a top gate is fabricated separately by stacking graphite on top of a thin hBN flake. The first half of the bilayer graphene flake is stacked beneath the top gate, and the other half is rotated by $\theta = 0.03^\circ$. Finally, the rotated graphene is stacked beneath the graphene on the top gate (Fig. 1e), which is then released onto the bottom gate on the pre-patterned chip (Fig. 1f).

After stacking the double-gated TDBG structure, a Hall bar etching mask with 1D graphene contacts is designed on a clean region of the device. The device is coated with PMMA 950K

A4 resist, and the etching mask is written using e-beam

lithography. Exposed graphite and hBN regions are etched completely using low-power O_2 and CHF_3/O_2 plasma, respectively. After the Hall bar geometry has been defined (Fig. 2a), the device is coated with PMMA 495K A4 and PMMA 950K A2 to write the electrode pattern connecting to the TDBG contacts. After writing the pattern using electron beam lithography, the exposed contact regions of the Hall bar are then etched completely to expose a 1D TDBG contact region.

Finally, chromium, palladium, and gold contacts are deposited onto the chip, and the remaining resist is removed in an acetone bath (Fig. 2b).

Results:

Sweeping the top and bottom gate voltages of the device at $T = 1.5K$ gave rise to gate- dependent signatures in the hole-doped region (Fig. 3a). This implies a gate-induced change in the structure being measured, in which graphene layers slide between a Bernal and rhombohedral stack ordering. By applying an external magnetic field, the magnitude of the switching response varies dramatically from the $B = 0T$ case. After applying an external field $B = 2T$, the switching response in the higher hole density region is emphasized, whereas the switching response closer to charge neutrality is emphasized in the zero-field case (Fig. 3a,c). Having defined part of the switching region, the measurement scheme demonstrated in Fig. 3b is conducted, in which the device switches deep into the rhombohedral phase. From the rhombohedral-dominated phase, two measurements of the switching response $R_{xx}(n, D)$ are made by ramping V_{tg} (V_{bg}) and then sweeping V_{bg} (V_{tg}) to map out the entire switching region. The sum of these plots highlights multiple boundaries in the hole-doped region (Fig. 3d). These distinct equipotential lines correspond to the free energy required to overcome the domain wall pinning energy to switch from one order to another.

Conclusions and Future Steps:

These results demonstrate the transport behaviors of domain switching in multi-layer 2D materials. Domain switching can be used to gain new insights into exotic transport phenomena. Future experiments may involve domain switching in platforms with different stacking configurations, twist angles, and crystals. It would also be of great interest to explore emergent transport properties unique to these different stacking orders and their interactions in a domain switching platform.

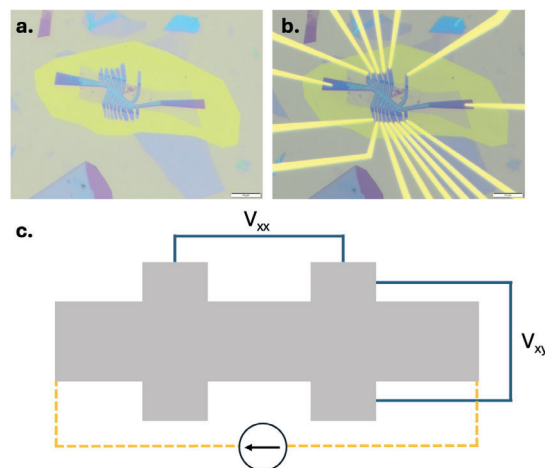


Figure 2: a, Complete stack (Fig. 1f) etched into a Hall bar geometry. b, Cr/Pd/Au contacts deposited on 1D TDBG contacts. c, Hall bar measurement configuration.

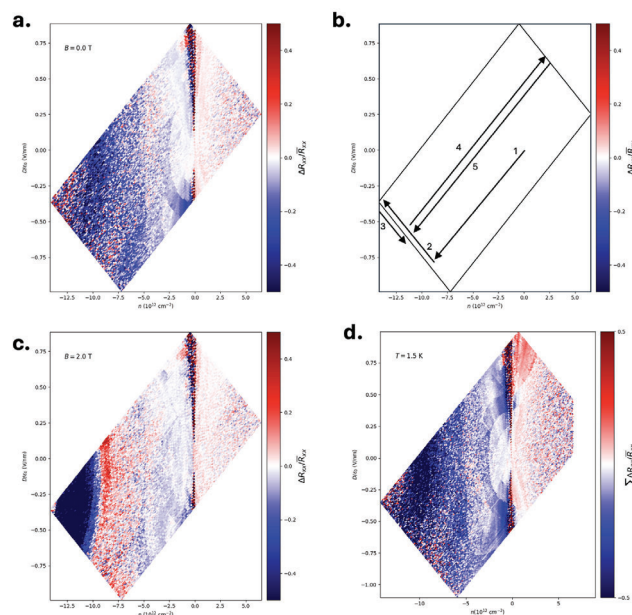


Figure 3: a, Switching boundary between Bernal and rhombohedral phases. This is defined by the mean normalized difference between the forward and backward bottom gate sweeps. b, Measurement scheme to define switching boundary in Fig. 3a. c, Same measurement as Fig. 3a under $B = 2T$. d, Sum of the mean normalized differences from the bottom and top gate sweeps. This plot maps the entire rhombohedral-Bernal switching region.

References:

- [1] K. S. Novoselov et al., Electric Field Effect in Atomically Thin Carbon Films. *Science* 306, 666-669 (2004). <https://doi.org/10.1126/science.1102896>
- [2] Lui, C., Li, Z., Mak, K. et al. Observation of an electrically tunable band gap in trilayer graphene. *Nature Phys* 7, 944-947 (2011). <https://doi.org/10.1038/nphys2102>
- [3] Electrode-Free Anodic Oxidation Nanolithography of Low-Dimensional Materials Li, H. et al. *Nano Letters* 2018 18 (12), 8011-8015 DOI: 10.1021/acs.nanolett.8b04166